Transactions of the Materials Research Society of Japan 26 [3] 1009-1012 (2001)

Ferroelectric Properties of Heteroepitaxial $PbZr_{0.5}Ti_{0.5}O_3$ Thin Films and Crystal Structure Close to the Interface

Yuko SAYA[A, B], Shunji WATANABE[A], Maki KAWAI[A*],
Takeshi HANADA[C] and Yoshihiko HIROTSU[C].

[A] RIKEN (Institute of Physical and Chemical Research), 2-1 Hirosawa, Wako, Saitama 351-0198, Japan

Corresponding author: Fax: 81-048-462-4663, e-mail address: maki@postman.riken.go.jp

[B] Department of Physics, Faculty of Science, Science University of Tokyo, 1-3 Kagurazaka, Shinjuku-ku, Tokyo 162-8601, Japan

[C] ISIR, Osaka University, 8-1 Mihogaoka, Ibaraki, Osaka, 567-0047, Japan

Abstract

$PbZr_{0.5}Ti_{0.5}O_3$ (PZT) thin films were successfully formed on a $YBa_2Cu_3O_{7-\delta}$ (YBCO) bottom electrode film epitaxially grown on a $SrTiO_3$(100) substrate by pulsed laser deposition. The piezoelectric properties of the thin PZT films measured by means of a scanning probe microscope (SPM) exhibited a hysteresis loop indicating the existence of "nonswitching regions" fixed in the direction of negative remanent polarization. The estimated effective thickness of the "nonswitching regions", based on the SPM measurement, was about 20 nm. Transmission electron microscope observation revealed that small crystalline grains of 10~20 nm size are formed close to the YBCO electrodes. Nanobeam electron diffraction and X-ray diffraction (XRD) patterns revealed that the small PZT grains were epitaxially grown, and *a* and *c* axes aligned normal to the surface coexisted.
KEYWORDS: ferroelectric properties, heteroepitaxial films, lattice strain, nonswitching regions.

1. INTRODUCTION

Ferroelectric material is attracting considerable interest, due to its applicability in such devices as nonvolatile ferroelectric random access memories [FeRAMs] and dynamic random access memories [DRAMs]. In particular, lead zirconate titanate [$Pb(Zr_xTi_{1-x})O_3$; PZT] is known as an excellent material for such device applications, because it shows superior ferroelectric and dielectric properties. One of the problems concerning the FeRAM device was fatigue, the decrease in polarization ability caused by repeated writing. This problem was solved by utilizing conductive oxide electrodes such as IrO_2, $SrRuO_3$, RuO_2, $La_{0.5}Sr_{0.5}CoO_3$ and $YBa_2Cu_3O_7$ (YBCO).[1]-[5] Since the origin of fatigue was oxygen vacancies created near the metal electrode,[6] oxide electrodes with good electrical conductivity functioned well to improve the fatigue performance of PZT thin films. The dielectric constant and remanent polarization of PZT thin films are known to decrease with decreasing thickness of ferroelectric films.[7] This degradation may be caused by the existence of different crystal structures, grain sizes and orientations in the vicinity of the electrode. In contrast, some theoretical reports based on thermodynamic calculations suggest that the two-dimensional compressive stress caused at the interface may improve the properties of ferroelectric material, such as increased Curie temperature (Tc) and coercive field (E_c), compared to those of the bulk.[8, 9] Such phenomena are expected to occur for heteroepitaxial thin films, which have lattice strain caused by lattice mismatch between the electrode material and the ferroelectric film. Actually, these theoretical forecasts have been experimentally confirmed in the case of $PbTiO_3$ and (Ba, Sr) TiO_3 thin films.[10-12] These results suggested that stress can improve the electrical properties, which is promising for future devices. For the application of future microelectronic devices, it is necessary to investigate the relationship between the stress caused by lattice mismatch and the ferroelectric properties at the vicinity of the interface. Therefore, it is important to investigate the interfacial crystal structure and electric properties of the ferroelectric materials.

In this study, heteroepitaxial PZT thin films were successfully prepared on atomically flat YBCO bottom electrode on a $SrTiO_3$(100) substrate, by the pulsed laser deposition (PLD) method. Using these films, piezoelectric properties were investigated by means of a scanning probe microscope (SPM), and the crystal structure was observed using a transmission electron microscope (TEM) and X-ray diffraction (XRD). Based on the result of observation, the relationship between interfacial lattice strain and electric properties is discussed.

2. EXPERIMENTAL

The substrate used was an atomically flat $SrTiO_3$(100) single crystal, treated with a combination of ultrasonic agitation and subsequent annealing at 1000℃ in air. A detailed explanation of this process has been given elsewhere.[13] Ferroelectric PZT(001) and YBCO films were formed by a PLD method. A 193 nm ArF excimer laser was focused onto polycrystalline targets of YBCO or lead-enriched PZT ($Pb(Zr_{0.5}Ti_{0.5})O_3$+15%PbO). The YBCO films were deposited using the laser fluence of about 3 J/cm^2 and the repetition rate of 1 Hz. The deposition was carried out at the substrate temperature of 635℃ under 0.5 Pa of oxygen atmosphere. The PZT films were deposited using the laser fluence of 4 J/cm^2 and

the repetition rate of 3 Hz. The PZT films were deposited on YBCO films at the substrate temperature of 510 ℃ under 0.1 Pa of nitrogen dioxide (NO_2). Nitrogen dioxide was used as an oxidant because it is sufficiently strong to oxidize PZT film at low pressure (0.1 Pa) at the PZT crystallization temperature (600°C). By reducing the NO_2 pressure and substrate temperature, as described above, flat and well-crystallized film surfaces were obtained.

Fundamental ferroelectric properties were investigated using an 80-nm-thick PZT film. Platinum/palladium alloy was deposited on the PZT films as a top electrode for the measurement of the dielectric and ferroelectric properties, where the shape of the electrode was a circle (0.2 mm in diameter). The dielectric constant and dissipation factors for PZT films were measured at room temperature with an inductance-capacitance-resistance meter at 1 kHz. D-E hysteresis loops were examined with a Sawyer-Tower circuit at 200 Hz. The dielectric constant was 500 and the dissipation factor was 0.03. The remanent polarization was 22 $\mu C/cm^2$, and the coercive field was 200 kV/cm.

Piezoelectric hysteresis loops of the PZT films were obtained with a SPM. The piezoelectric hysteresis loops can be obtained by detecting the piezoelectric response caused by an oscillating voltage applied between the tip and the bottom YBCO electrode, with the PZT films polarized in advance. The amplitude was 1 V_{p-p} ac, and the repetition rate was 2 kHz. The piezoelectric response of the PZT films can be measured in the form of the $A\cos\phi$ signal. The amplitude of A is proportional to the magnitude of remanent polarization. The phase difference ϕ shows the direction of polarization. If the piezoelectric response signals $A\cos\phi$ are plotted as a function of the dc poling voltages applied, piezoelectric hysteresis loops can be drawn. Details of the measurement method have been reported elsewhere.[14]

The crystal structure of the deposited films was analyzed by XRD using CuKα radiation. The cross-sectional TEM observations were carried out with JEM-3000F operating at 300 keV. A nanobeam electron diffraction (NBD) pattern was obtained using a probe diameter of 23-80 nm.

3. RESULTS AND DISCUSSION

3.1 Piezoelectric properties of the PZT thin films

The piezoelectric properties of the PZT thin films prepared were observed by means of SPM. Figure 1 shows the piezoelectric hysteresis loops for the 80-nm-thick PZT film, where the hysteresis loop shows an asymmetric shift toward negative remanent polarization. On the other hand, in the hysteresis curve of the 160-nm-thick film, the amplitude of asymmetry was reduced. The asymmetric ferroelectricity could be due to the existence of "nonswitching regions" induced by the lattice strain between the PZT film and the YBCO electrode.[12], [15] The effective thickness of the "nonswitching regions" in the PZT films was estimated from the asymmetry of the hysteresis loops. Expressing the amplitude for the negative poling and the positive poling as A(-) and A(+), respectively, the ratio of A(-)/A(+) was 2/1 in the case of the 80-nm-thick PZT film. The "nonswitching regions" were estimated to be one-fourth of the total thickness, as shown in Fig. 2. That is to say, the

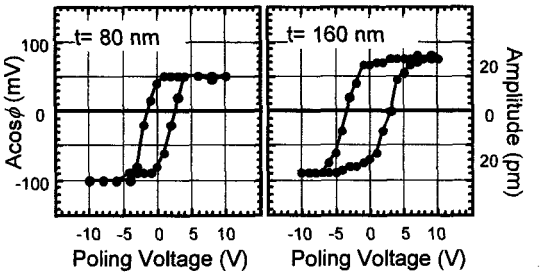

Fig. 1. Piezoelectric hysteresis loops for the PZT films epitaxially grown on a YBCO(100)/$SrTiO_3$(100) heterostructure substrate. The hysteresis loops were asymmetric, where the amplitude ratio of A(-)/A(+) was 2/1 for the 80-nm-thick film and 4/3 for the 160-nm-thick film, respectively.

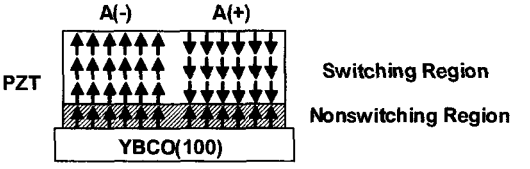

Fig. 2. Schematic of the 80-nm-thick PZT film with switching and nonswitching regions directed toward negative polarization at the PZT/YBCO interface. Since the ratio of A(-)/A(+) in piezoelectric hysteresis loops was 2/1, the nonswitching region was estimated to be one-fourth the total thickness.

estimated effective thickness of the "nonswitching regions" was about 20 nm.

3.2 Crystal structure of the PZT thin films

3.2.1 Thickness dependence on the XRD pattern of PZT films: The structure of $Pb(Zr_{0.5}Ti_{0.5})O_3$ is tetragonal perovskite at room temperature with the lattice constants a=b=0.403 nm and c=0.411 nm, whereas $YBa_2Cu_3O_{7-}$ has orthorhombic structure with a=0.382 nm, b=0.389 nm and c=1.170 nm (c/3=0.390 nm) at room temperature. We have deposited $Pb(Zr_{0.5}Ti_{0.5})O_3$ films with the thickness from 60 nm to 160 nm on the YBCO bottom electrode film by the PLD method. The XRD patterns revealed that the YBCO bottom electrode, the thickness of which was 50 nm, was preferentially a-axis-oriented normal to the surface and that the lattice constant of the a-axis was 0.387 nm.

The θ-2θ scan in X-ray diffraction exhibited strong peaks of the tetragonal $Pb(Zr_{0.5}Ti_{0.5})O_3$ perovskite structure for all the films observed. For the PZT films over 160 nm thick, the lattice constant was about 0.407 nm, independent of the thickness. The value observed here did not coincide with that known for the a-axis or the c-axis value of the bulk PZT, rather, the intermediate value indicates a pseudocubic structure.

The thickness dependence of the PZT film on the peaks is examined. The XRD patterns for the films with thickness from 60 to 160 nm are shown in Fig. 3, and give the mean lattice constant. As the thickness of the film decreases, the peak shifts toward the low 2θ angle, that is, the mean lattice constant of the vertical axis becomes larger. Since the in-plane lattice constant of the bottom electrode YBCO(100) (a=0.382, b=0.389 nm) is smaller

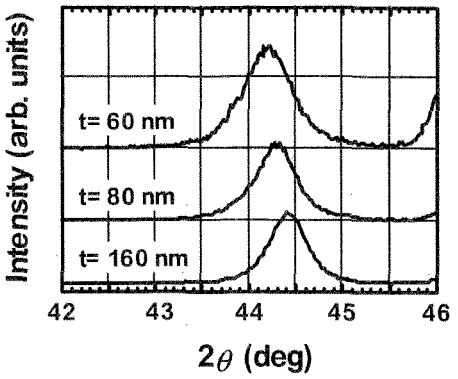

Fig. 3. Thickness dependence of XRD patterns for peaks of the PZT films grown on the YBCO(100) bottom electrodes. The vertical lattice constant increased due to the lattice mismatch between PZT and YBCO, and the effect was enhanced in the case of thin PZT films.

than that of the PZT(001) (a=b=0.403 nm), it is expected that two-dimensional stress will appear due to the lattice mismatch in the heteroepitaxial PZT films at the interfacial region near the bottom electrode. Because such an effect should appear in the region close to the interface, the contribution of stressed region in the thin film is larger than that in the thick film. The observed change in the lattice constants should reflect the existence of lattice strain close to the interface.

3.2.2 TEM Observation: Figure 4 shows a cross-sectional bright-field TEM image of the PZT (80 nm)/YBCO /STO(100). Close to the PZT/YBCO interface, small crystal grains of size 10~20 nm are formed up to the thickness of ~20 nm, beyond which larger crystal grains are observed, suggesting that the growth of PZT films is in the Volmer-Weber mode. Figure 5 shows a NBD pattern obtained with a 80-nm-diameter probe near the PZT/ YBCO interface. The NBD pattern clearly shows two diffraction origins, one from YBCO(100) and the other from PZT. For the YBCO diffraction pattern, a threefold periodic pattern, which is expected for the normal YBCO structure, is not clearly observed in either in-plane or vertical diffraction patterns. This suggests that the

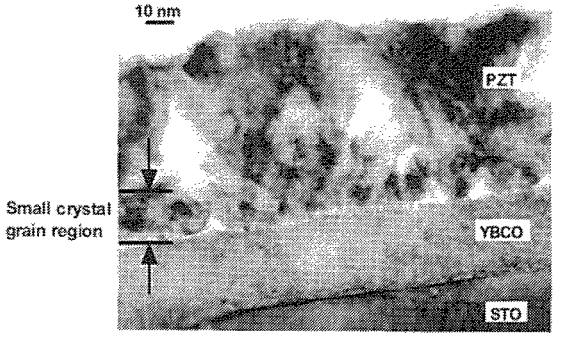

Fig. 4. Cross-sectional bright-field TEM image of $PbZr_{0.5}Ti_{0.5}O_3$ (80 nm)/$YBa_2Cu_3O_{7-\delta}$ heteroepitaxial thin films, grown on a $SrTiO_3$(100) substrate. The crystal grains of 10~20 nm in size grew and come into contact with adjacent grains close to the interface.

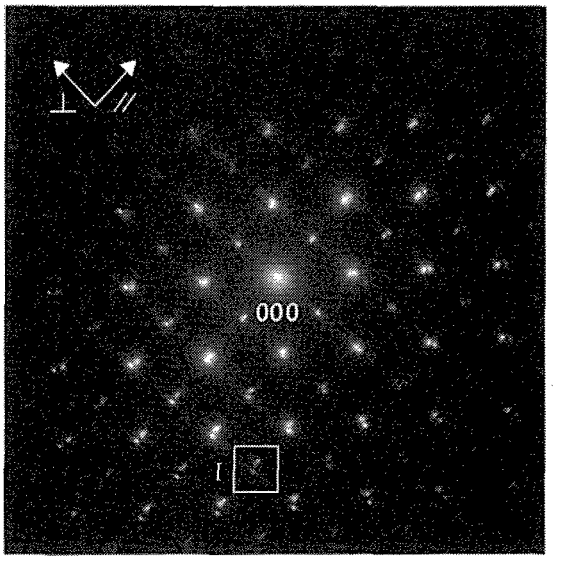

Fig. 5. Nanobeam electron diffraction near the interface between the PZT films and YBCO bottom electrode, using 80-nm-diameter probe

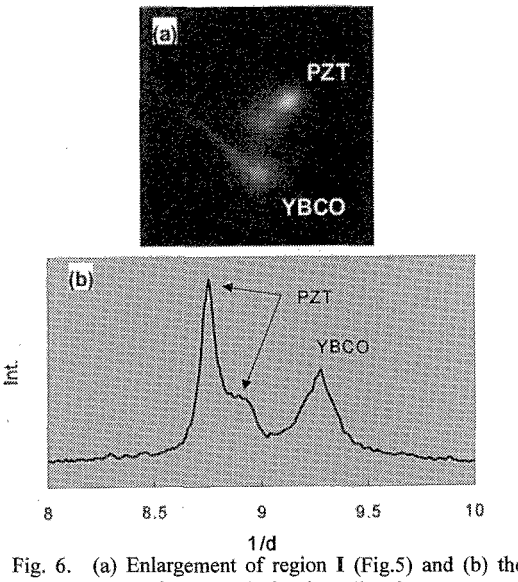

Fig. 6. (a) Enlargement of region **I** (Fig.5) and (b) the diffraction intensity along the in-plane direction.

deposited YBCO film in the present case resembles cubic-YBCO.[16] The superimposed diffraction patterns for the PZT film and the YBCO bottom electrode indicate that the film is grown in a cube-on-cube manner with lattice mismatch of less than 4 %. An enlargement picture of region **I** and the diffraction intensity along with the in-plane direction are shown in Fig. 6(a) and Fig. 6(b), respectively. Here, the diffraction spots split into two along the in-plane direction. The split spots suggest that there are two kinds of lattice constants, small and large. Assuming that the lattice constants of the prepared YBCO thin films are the same as those of the cubic-YBCO (a=b=c=0.386 nm),[16] the two kinds of lattice constants are similar to the a- and c-axis values of bulk PZT lattice constants, that is, the a- and c-axis lattice constants coexist in-plane. On the other hand, in the XRD result, the vertical lattice constant of the PZT films with 60 nm

thickness is larger than the *a*-axis value of bulk PZT. This is probably because the *c*-axis preferentially aligns vertically in the vicinity of the interface of the YBCO bottom electrode, in the context of epitaxial growth. Therefore, it can be considered that for the small PZT grains of 10~20 nm size near the interface, the *c*-axis is preferentially aligned along the surface normal, although *a*-axis-oriented grains also exist in this region. The reason why peaks of neither the *a*- or *c*-axis were observed by XRD is probably due to the fact that the domain size of each grain is less than the coherent length of XRD, which is known to be ~100 nm. Under the existence of strain caused by lattice misfit with YBCO, the PZT crystal could not grow into large domains in the vicinity of the interface, and the large relaxed crystallites started to grow beyond the interfacial region towards the surface region. Since the estimated thickness of the "nonswitching regions" was ~20 nm, based on SPM measurement and which is similar to the thickness in the region of grains of PZT, it is concluded that the "nonswitching regions" are caused by the lattice strain at the interface between the PZT film and YBCO electrode.

In the present study, the asymmetry in a PZT unit cell, which is expected to be the cause of "nonswitching regions" described in the previous report,[15] was not observed. The asymmetric hysteresis loops may be due to other causes such as the imprint phenomenon resulting from charged defects[17] and the different work functions of the top and bottom electrodes.[18] The reason why these stress layers behave as "nonswitching regions" with negative remanent polarization still remains to be solved. Further studies on the effect of different electrodes with different lattice constants and work functions will be carried out.

4. CONCLUSION

$PbZr_{0.5}Ti_{0.5}O_3(001)/YBa_2Cu_3O_{7-\delta}$ heteroepitaxial thin films were successfully grown on a $SrTiO_3(100)$ substrate by PLD. Using these PZT films, we investigated the electrical properties using the SPM and the crystal structure by XRD and TEM. The SPM measurement revealed that 80-nm-thick PZT films had asymmetric piezoelectric hysteresis loops indicating the existence of "nonswitching regions" with a negative remanent polarization. The thickness of "nonswitching regions", estimated from the SPM measurement, was about 20 nm. The corresponding thickness at the interface between the bottom electrode and the PZT film was revealed to show two-dimensional stress. TEM observation close to the interface between YBCO and PZT showed that small PZT crystal grains with the size of 10~20 nm are formed up to the film thickness of ~20 nm. The XRD and NBD patterns indicated that the *a* and *c* axes coexist along the in-plane direction, where the *c*-axis orientation was preferentially observed in the XRD at the interface.

ACKNOWLEDGEMENTS

The present study is partly supported by the "Special Coordination Funds for Promoting Science and Technology (SCF)" from the Science and Technology Agency of Japan.

REFERENCES

[1] T. Nakamura, Y. Nakao, A. Kamisawa and H. Takasu: Appl. Phys. Lett. **65** (1994) 1522.
[2] H. Fujisawa, S. Nakashima, K. Kaibara, M. Shimizu and H. Niu: Jpn. J. Appl. Phys. **38** (1999) 5392.
[3] G. E. Pike, W. L. Warren, D. Dimos, B. A. Tuttle, R. Ramesh, J. Lee, V. G. Keramidas and J. T. Evans, Jr: Appl. Phys. Lett. **66** (1995) 484.
[4] A. Gruverman, O. Auciello and H. Tokumoto: Appl. Phys. Lett. **69** (1996) 3191.
[5] R. Ramesh, W. K. Chan, B. Wilkens, H. Gilchrist, T. Sands, J. M. Tarascon, V. G. Keramidas, D. K. Fork, J. Lee and A. Safari: Appl. Phys. Lett. **61** (1992) 1537.
[6] T. Mihara, H. Watanabe and C. A. Paz de Araujo: Jpn. J. Appl. Phys. **33** (1994) 3996.
[7] Y. Sakashita, H. Segawa, K. Tominaga and M. Okada: J. Appl. Phys. **73** (1993) 7857.
[8] G. A. Rossetti, Jr., L. E. Cross and K. Kushida: Appl. Phys. Lett. **59** (1991) 2524.
[9] B. Qu, W. Zhong and P. Zhang: Ferroelectrics **197** (1997) 27.
[10] H. Uchida, A. Sakita, N. Wakiya, K. Shinozaki and N. Mizutani: J. Ceram. Soc. Japan. **108** (2000) 21.
[11] K. Abe, S. Komatsu, N. Yanase, K. Sano and T. Kawakubo: IEICE Trans. Electron. **E81-C** (1998) 505.
[12] K. Abe, S. Komatsu, N. Yanase, K. Sano and T. Kawakubo: Jpn. J. Appl. Phys. **36** (1997) 5575.
[13] K. Iwahori, S. Watanabe, T. Komeda, M. Kawai, A. Saito, Y. Kuwahara and M. Aono: Jpn. J. Appl. Phys. **38** (1999) 3946.
[14] Y. Saya, S. Watanabe, T. Komeda, M. Kawai, H. Yamada and K. Matsushige: Jpn. J. Appl. Phys. **39** (2000) 3799.
[15] K. Abe, S. Komatsu, N. Yanase, K. Sano and T. Kawakubo: Jpn. J. Appl. Phys. **36** (1997) 5846.
[16] T. Nagano, T. Hashimoto and J. Yoshida: Physica C **265** (1996) 214.
[17] S. H. Kim, D. S. Lee, C. S. Hwang, D. J. Kim and A. I. Kingon: Appl. Phys. Lett. **77** (2000) 3036
[18] P. W. M. Blom, R. M. Wolf, J. F. M. Cillessen and M. P. C. M. Krijn: Phys. Rev. Lett. **73** (1994) 2107.

(Received January 29, 2001; Accepted February 16, 2001)